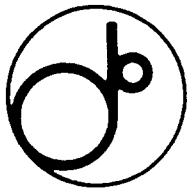


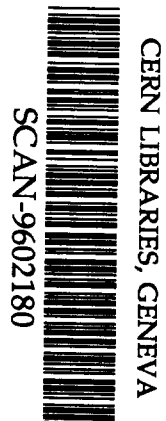
LL



KEK Preprint 95-107
September 1995
A/M/R

Synchrotron Radiation Damage Test of Insulating Materials in the TRISTAN MR

H. Mitsui, R. Kumazawa, T. Tanii, T. Chugun
Y. Ohsawa, T. Ozaki, and K. Takayama



SW9610

submitted to "Particle Accelerators"

National Laboratory for High Energy Physics, 1995

KEK Reports are available from:

Technical Information & Library
National Laboratory for High Energy Physics
1-1 Oho, Tsukuba-shi
Ibaraki-ken, 305
JAPAN

Phone: 0298-64-5136

Telex: 3652-534 (Domestic)
(0)3652-534 (International)

Fax: 0298-64-4604

Cable: KEK OHO

E-mail: Library@kekvox.kek.jp (Internet Address)

SYNCHROTRON RADIATION DAMAGE TEST OF INSULATING MATERIALS IN THE TRISTAN MR

H.Mitsui,R.Kumazawa,T.Tanii and T.Chugun

Toshiba Corporation

2-4 Suchiro-cho,Tsurumi-ku,Yokohama-shi,230 Japan

Y.Ohsawa,T.Ozaki,and K.Takayama

National Laboratory for High Energy Physics in Japan(KEK)

1-1,Oho,Tsukuba-shi,Ibaraki-ken,305 Japan

Abstract

An irradiation test of typical insulating materials for an accelerator magnet was carried out, using actual radiation in the TRISTAN MR(main ring) which is operated at the quite high level of radiation. Physical and chemical degradations of the insulating materials due to irradiation were systematically studied. The effects of insulating materials, combinations thereof and insulation manufacturing processes on the irradiation degradation are discussed.

1.INTRODUCTION

TRISTAN is an e^+e^- colliding beam accelerator with the collision energy in a range of $\sqrt{S} \approx 60$ GeV. The MR was operated first in October 1986 at a beam energy of 25 GeV. Since then the beam energy has been increased step by step from 25 GeV to 30 GeV by employing RF accelerating cavities [1]. Thereafter the radiation damage on accelerator components, such as signal cables for beam monitors, power cables for vacuum pumps, various electric circuit components, and magnet coil insulations has become increasingly serious [2].

Systematic studies of the radiation damage on electrical insulating materials used for particle accelerators are found in the literatures [3,4]; meanwhile, the same kind of tests were carried out in the

TRISTAN MR [5] several years ago. However, radiation damage beyond 100MGy is a current big concern in the accelerator society because irradiation beyond 100 MGy is likely in localized regions of existing machines. Under such conditions, up to this dose level, other properties than mechanical have been systematically tested on the three types of insulating materials and the results are compared with each other.

2.SPECIMENS

Three types of insulating materials for a magnet coil, as shown in Table 1, were chosen for the current study. Type A is the so-called vacuum-pressure-impregnation(VPI) insulation system which consists of glass-cloth reinforced mica-paper tape impregnated with epoxy resin. Type B is a resin-rich insulation system which is manufactured in the atmosphere, by molding bismaleimide triazine(BT) resin preimpregnated glass-cloth, and by heat shrinkable tape. Type C is another resin-rich insulation system which is manufactured in a vacuum, by molding polyimide preimpregnated glass-cloth with an asphalt compound.

For the purpose of detecting a change in their electrical properties such as $\tan \delta$, insulation resistance, and breakdown voltage(BDV), an aluminum bar with a cross-section of 6(mm)x25(mm) and total length of 160(mm) was covered with each of these materials in the same manner as actual coils. To measure a change in their mechanical properties, on the other hand, samples were formed in a laminate by molding the tapes in the same manufacturing process as that of the bar coils. The plate sizes were 2 mm in thickness, 25 mm in width and 100 mm in length.

3.EXPERIMENTAL METHODS

3.1.Test bench

All of the test specimens were put in a radiation box located in the steering magnet of the

normal section where the dose rate of $3.7\text{-}6.5 \times 10^4$ Gy/h, consisting of direct synchrotron radiation and its secondary, was very high in the MR. The dose has been calibrated with the thermo-luminescence dosimeter method [2] by employing a test beam with well monitored energy and current. Number of samples per test, material and dose was three, because of the limitation of the irradiation space.

The samples taken out of the irradiation box at some fixed time period were subjected to the tests explained in the following. Measurements of insulation resistance and $\tan \delta$ at high temperatures were done, in order to know the informations on the degradatio which cannot obtain from the data at room temperature.

3.2. Electrical insulation tests

(1) Insulation resistance: The property was measured at 1 kV dc. One minute value was made as the measurement value.

(2) $\tan \delta$ and capacitance: $\tan \delta$ and capacitance were measured at 50Hz by using a high voltage auto schering bridge (Soken Electric Co., Ltd. type: DAC-HAS-3).

(3) BDV: 50 Hz ac BDV was measured by the continuous voltage rising method in 0.5 kV/s for a specimen as shown in Fig. 1.

3.3. Flexural tests

Flexural tests were carried out by using a universal materials testing machine (Instron Ltd. type: 1186) on specimens with a thickness of about 2 mm. The span distance was 30 mm and the bending speed 0.5 mm/min in a three point bending method. Flexural strength and modulus were obtained.

3.4. FT-IR analysis

Fourier Transform Infrared Spectrometer (FT-IR) analysis was done by the KBr method for the powder obtained by filing the surfacial portion of samples, in order to survey the change in chemical composition.

3.5. SEM observation

Surface and cross-section of bar coils and laminates were observed by a scanning electron microscope (SEM).

3.6. Water content

Water content of the specimens were measured by the Karl Fischer's method.

4. TEST RESULTS AND DISCUSSIONS

4.1. Relationship between dose and electrical insulation properties.

In Fig. 1, the magnitude of BDV of the bar coils are shown as a function of dose. For all three sample types BDV decreases with the increase of dose. At 167 MGy the order is $A > C > B$. The fact that type A with epoxy resin was higher than type B and C with polyimide resin, which is generally superior to epoxy resin in radiation resistance, may be due to the presence of mica. Comparing type B with type C which are the glass-cloth reinforced resin-rich insulations without mica, type C is apparently superior to type B with respect to the BDV as seen in Fig. 1. This can be attributed to the existence of voids in the insulating materials. The oxidation tends more to develop in the void containing insulating materials than in the void-free ones. Type C is void-free because it was processed in a vacuum by the asphalt-compound molding technique. Type B was processed in the atmosphere by the heat shrinkable tape molding; therefore it contains voids. It should be pointed out that in the type B sample voids generate more easily than in type C with irradiation as discussed below.

Fig. 2 shows the relationship between dose and $\Delta \tan \delta$, where, $\Delta \tan \delta = (\tan \delta @ 3kV - \tan \delta @ 0.5kV)$. The parameter $\Delta \tan \delta$ is known to reflect partial discharges in a void, so it is reasonable to regard $\Delta \tan \delta$ as a measure of the amount of voids. The $\Delta \tan \delta$ increases at a smaller dose in type B than in type C. This suggests that gases evolved by radiation decompositions of the resin induce the delaminations of the insulating materials [6]. The reduction in $\Delta \tan \delta$ at 167 MGy for type B could be due to a puncture of the insulation caused by the increase of pressure in the closed void and hence the void became open to the atmosphere resulting in a decrease in volume.

Figs. 3 and 4 show the relationship between dose and insulation resistance, as a function of measuring temperature for type A and type B, respectively. In type A, at temperatures above 120 °C the insulation resistance decreases with the increase of dose. On the other hand, in type B, though the insulation resistance decreases with the increase of dose, it recovers up to the initial level above 100°C at 167 MGy. In the analysis by FT-IR, no remarkable change in chemical structures could be found after the measurements of insulation resistance at high temperatures. As shown in Table 2, the water absorption content increased with the increase of dose. In type B, though the insulation resistance decreased with the increase of dose due to the absorbed water, the water should be released by heating, resulting in the recovery of insulation resistance, where voids might be opened at 167 MGy. On the other hand, in type A, it is supposed that most voids still were not opened to the atmosphere due to mica as a barrier, and therefore the insulation resistance did not recover.

These phenomena, to recover the insulation characteristics at temperature above 100°C at 167 MGy, were also found in $\tan \delta$. Figs. 5 and 6 show the relation between dose and $\tan \delta$ of type A and type B, respectively. In type B, $\tan \delta$ increases at temperatures above 100°C, with the increase of dose, however, it decreases down to the unirradiated level after 167 MGy. In type A, such the recovery phenomena were not found whereas the same phenomena as in type B were also found in type C. Both types B and C are the resin reinforced with only glass-cloth and it is supposed that voids in the resin progressively opened to the atmosphere once the insulation is delaminated.

4.2. Relationship between dose and mechanical properties.

Fig.7 shows the relationship between dose and flexural strength. Flexural strength begins to decrease remarkably above about 4 MGy in type A and above about 15 MGy in type B. In type C, flexural strength decreases gradually up to about 15 MGy, then decreases more rapidly down to 167 MGy. The degradation starting dose and decreasing tendency of the flexural strength are differentiated by the combination of matrix resin and reinforcement. The flexural strength at 167 MGy is higher in insulation type C then type B and is remarkably low in type A. The reason why type A was the

weakest would be the radiation degradation of matrix resin, which induces the decrease of interfacial adhesive strength between the resin and the mica and glass-cloth reinforcements, in addition to the gas pressure effect as mentioned above. This can also be deduced from the facts that the starting dose for the decrease in flexural strength is nearly the same as the starting dose for the increase of the thickness shown in Fig. 8 and the starting dose for the decrease of the flexural modulus in Fig. 9. On the other hand, type B and C show little change in the insulation thickness and flexural modulus, perhaps because of their open void system, as mentioned above.

4.3. Relationship between the observation by SEM and electrical and mechanical properties.

Fig. 10 shows the cross-sectional views of coil insulations by SEM for the unirradiated and 167 MGy irradiated specimens. Fig.10 (b) shows that, in type A, less degradation is found in the mica layer, whereas in comparison the resin in the vicinity of glass-fibers is severely deteriorated. It is assumed that this is the reason why in type A, the BDV was relatively high, although the flexural strength was the lowest. In type B, voids are locally found even in the unirradiated specimens as shown in Fig.10 (c) and, at 167 MGy, the resin around the glass fibers is whitened, as shown in Fig.10 (d). This whitened part increased with the increase of the dose, as a result of the increase of voids. This result agrees well with the tendency of $\Delta \tan \delta$ to increase. Moreover, voids stretch in the thickness direction, as shown in Fig. 10(d). This could be the reason why, in type B, the BDV was the lowest, although there was no great swelling in the insulation. In type C, almost no voids was observed in unirradiated specimens, as shown in Fig. 10 (e). However, at 167 MGy, damage is seen in the resin around the glass-fibers, like in type B, and voids are formed as shown in Fig.10 (f). This is supposed that the BDV decreased remarkably at 167 MGy. Fig.11 shows the appearance of the two flexural test samples for each type with the dose of 167 MGy. Dotted swellings are observed in type A, however, no such swellings are observed in type B and C. The reason of such differences could be due to the case by which gas evolved by irradiation to pass through the insulation. Further, the adhesive strength between the resin and the reinforcement is dominant factors which can influence the irradiation

degradation of the insulation.

4.4. Comparison of degradation starting dose between electrical and mechanical properties.

In the insulation degradation by the irradiation, the fact that in general mechanical properties degrade faster or primarily responsible for radiation damage is supported by experiments and operational experience; therefore it is also the basis for standardization of radiation test of insulating materials[6,7]. From this point of view, a comparison of the starting dose of the decrease in electrical and mechanical properties was made in this experiment.

Fig. 12 shows the residual BDV and flexural strength as a function of dose. In this figure, only type C agrees well with the above-mentioned experience[6,7]. In type A, both properties start to decrease at almost the same dose. In type B, it is noticeable that the mechanical property starts to decrease at a larger dose than the electrical property. Table 3 shows the dose to reduce the initial property of the breakdown strength and the flexural strength to half. Such criteria are usually used for the life expectation of the insulation, and the dose is defined as an index for radiation resistance of these insulations[7].

4.5. FT-IR analysis.

Fig. 13 shows the relation between dose and carbonyl absorbance appeared in the region of $1650 \sim 1800 \text{ cm}^{-1}$. Their relations are similar for all specimens. As seen in Figs. 2 and 13, the characteristics of samples for carbonyl absorbance qualitatively coincides with that for $\Delta \tan \delta$. Thus, the carbonyl absorbance can be a good degradation index in the same insulation. The carbonyl compounds are originated from the oxidation reactions caused by radiation. With the advance of oxidation reactions, ketone, aldehyde, carboxylic acid, etc. are formed on the polymer molecules in resins, which are responsible to carbonyl absorbance. The aldehyde and carboxylic acid are the polymer chain scission products. These oxidation products increase the $\tan \delta$ as well known. The oxidated products are liable to absorb water, Therefore, water absorption contents of coil insulations increased with increase of dose as seen in Table 2, and that the decrease of electrical insulation

properties are accordingly accelerated.

The authors reached the conclusion that these oxidation reactions also contribute the degradation of the insulating materials, and thus decreased BDV and flexural strength; the voids took essential roles in the process.

5. CONCLUSIONS

From the irradiation tests of typical insulating materials for magnet coils, using actual radiation in the TRISTAN MR (up to 167 MGy at the highest), the following conclusions can be drawn.

- (1) Epoxy/glass-cloth/mica-tape insulation processed by the VPI method has a higher BDV due to the presence of the mica tape; however its flexural strength degrades considerably at the higher dose.
- (2) The insulation processed by the asphalt pressure molding method in a vacuum is far superior both in electrical stability and mechanical rigidity to the insulation processed by the heat-shrinkable tape molding method.
- (3) The insulation processed by the heat-shrinkable tape molding method shows that the decrease in the BDV appears at a lower dose than for the flexural strength; this fact is contrary to common experience.
- (4) The ability to absorb wets in the coil insulation increases with the progress of the degradation.
- (5) The results observed by microscope are closely related to the electrical and mechanical properties.
- (6) Carbonyl absorbance is a useful index to measure the oxidation degradation of resins caused by radiation.
- (7) The radiation degradation of the tested samples is understandable by the assumption that the resin placed adjacently to the glass-cloth is decomposed to produce gases, which make the voids in resin matrix.

As a concluding remark, studies of the manufacturing process as well as the insulating materials themselves are, indeed, important in order to develop the higher radiation-resistant insulation. In

addition, because the measured absorbed dose of TRISTAN MR magnet coil exceeded 10MGy at the highest[8], so the authors anticipate that some of the coils will reach to the end of life in the near future, based on the data mentioned here.

REFERENCES

1. Y.Kimura and H.Baba, Proc.the 6th Sym. on Accelerator Science and Technology, 15(Tokyo,1987).
2. T.Momose,H.Hirayama,T.Ieiri,K.Takayama,Y.Ohsawa,K.Endo,H.Ishimaru,Y.Mizumachi,S.Takeda, T.Kawamoto, and K.Uchino, Proc. of the European Part. Accel. Conf.,1284(Rome,1988).
3. P.Beynel,P.Maier,and H.Schönbacher, CERN 82-10(1982).
4. G.Lipták,R.Schulcr,P.Maier,H.Schönbacher,B.Haberthür,H.Müller,andW.Zeier,CERN85-2(1985)
5. T.Ozaki,K.Takayama,Y.Ohsawa,T.Kubo,K.Endo,M.Hirano,T.Chugun,R.Kumazawa,and H.Mitsui, Proc. Part. Accel. Conf.,2015(1989)
6. IEEJ,Insulating Materials Irradiation Investigation Special Committee Report,Part I No.79(1967),(in Japanese).
7. IEC 544-2 Second edition (1991).
8. K.Endo and Y.Ohsawa,Radiation, **21, 2, 32** (1995),(in Japanese).

TABLE 1 Insulation constitution of test specimens.

Type	Material	Manufacturing process	Applied machine
A	Epoxy/mica/ E glass	Vacuum-pressure-impregnation	TRISTAN main ring
B	BT resin/ S glass	Heat shrinkable tape-molding	PS ring
C	Polyimide/ T glass	Asphalt-compound molding under vacuum	None

E glass : Electric grade glass

S, T glass : Boron-free glass

TABLE 2 Water contents of bar coil insulation (type B).

Dose (MGy)	0*	7	15	50	167
Water content (%)	0.41	0.49	0.49	0.79	0.81

*) original(unirradiated)

TABLE 3 Dose at half BDV and half flexural strength obtained from Fig.12.

Type	BDV	Flexural strength
A	3.3×10^7 Gy	1.9×10^7 Gy
B	4.6×10^7 Gy	1.1×10^8 Gy
C	1.1×10^8 Gy	1.3×10^8 Gy

Figure captions 21, 2,

Fig.1 BDV of bar coils vs. dose.

Fig.2 $\Delta \tan \delta$ of bar coils vs. dose.

Fig.3 Insulation resistance vs. dose(type A).

Fig.4 Insulation resistance vs. dose(type B).

Fig.5 $\tan \delta$ of bar coils vs. dose(type A).

Fig.6 $\tan \delta$ of bar coils vs dose(type B).

Fig.7 Flexural strength of laminates vs. dose.

Fig.8 Thickness of laminates vs. dose.

Fig.9 Flexural modulus of laminates vs. dose.

Fig.10 Cross-sectional photographs taken by a SEM

(a)unirradiated sample(type A, $\times 200$)

(b)167MGy irradiated sample(type A, $\times 200$)

(c)unirradiated sample(type B, $\times 60$)

(d)167MGy irradiated sample(type B, $\times 60$)

(e)unirradiated sample(type C, $\times 60$)

(f)167MGy irradiated sample(type C, $\times 60$)

Fig.11 Appearance of laminates after 167 MGy irradiation.

Fig.12 Residual BDV and flexural strength obtained from the results shown in Fig.1 and Fig.7.

Fig.13 Carbonyl absorbance vs. dose.

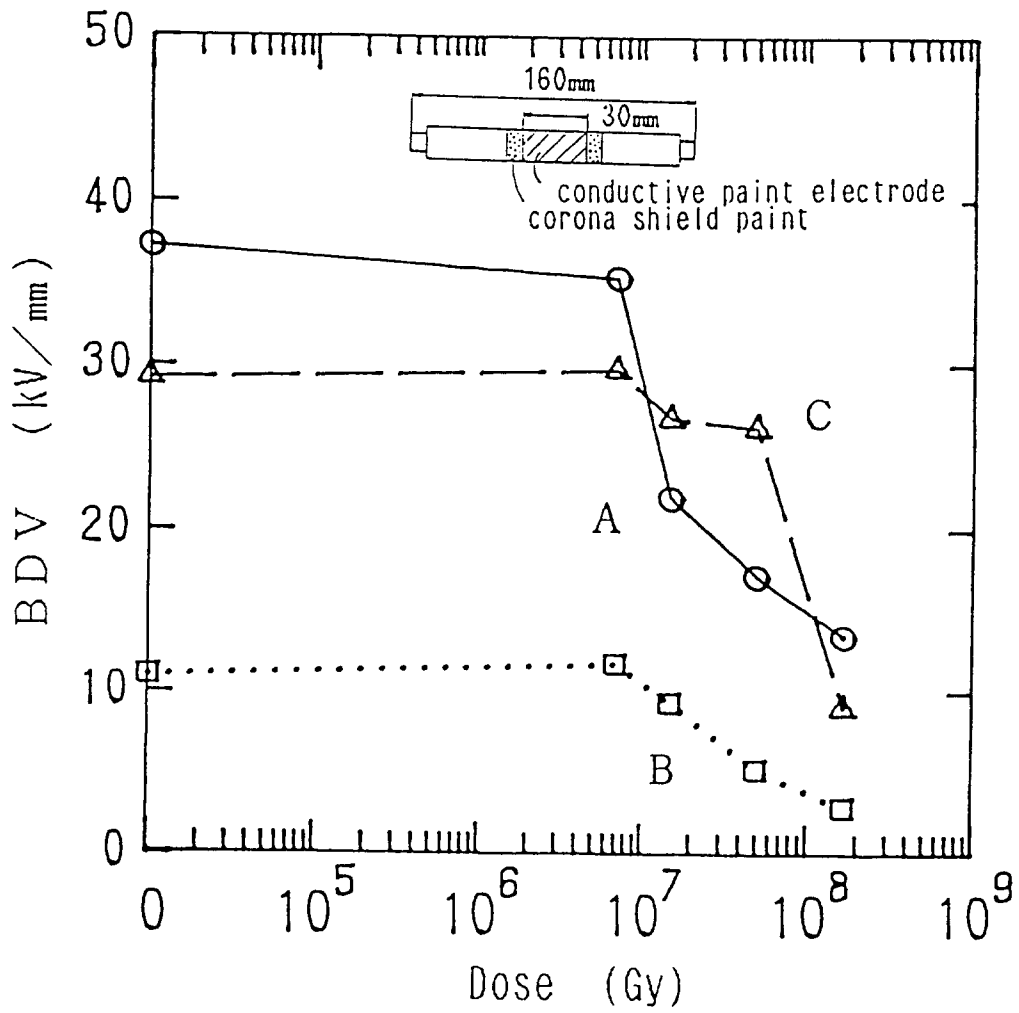


Fig.1 BDV of bar coils vs. dose.

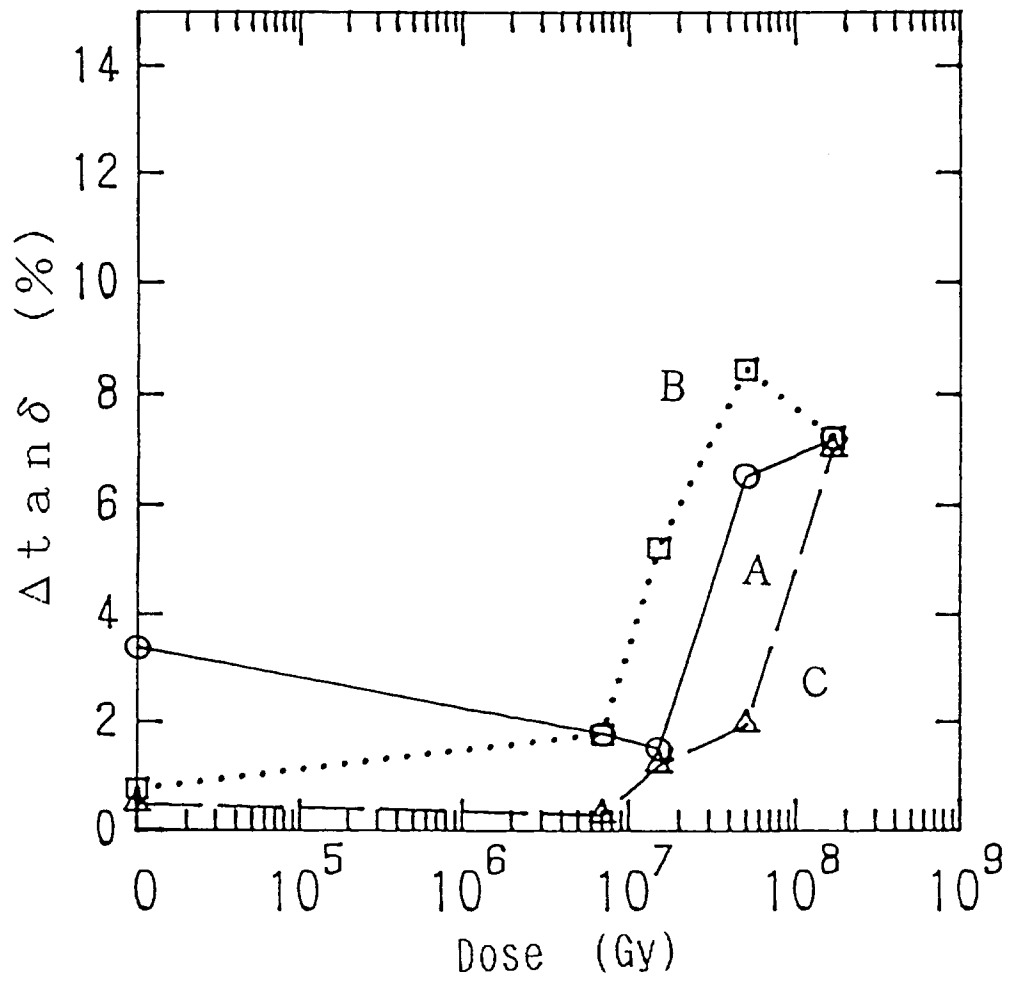


Fig.2 $\Delta \tan \delta$ of bar coils vs. dose.

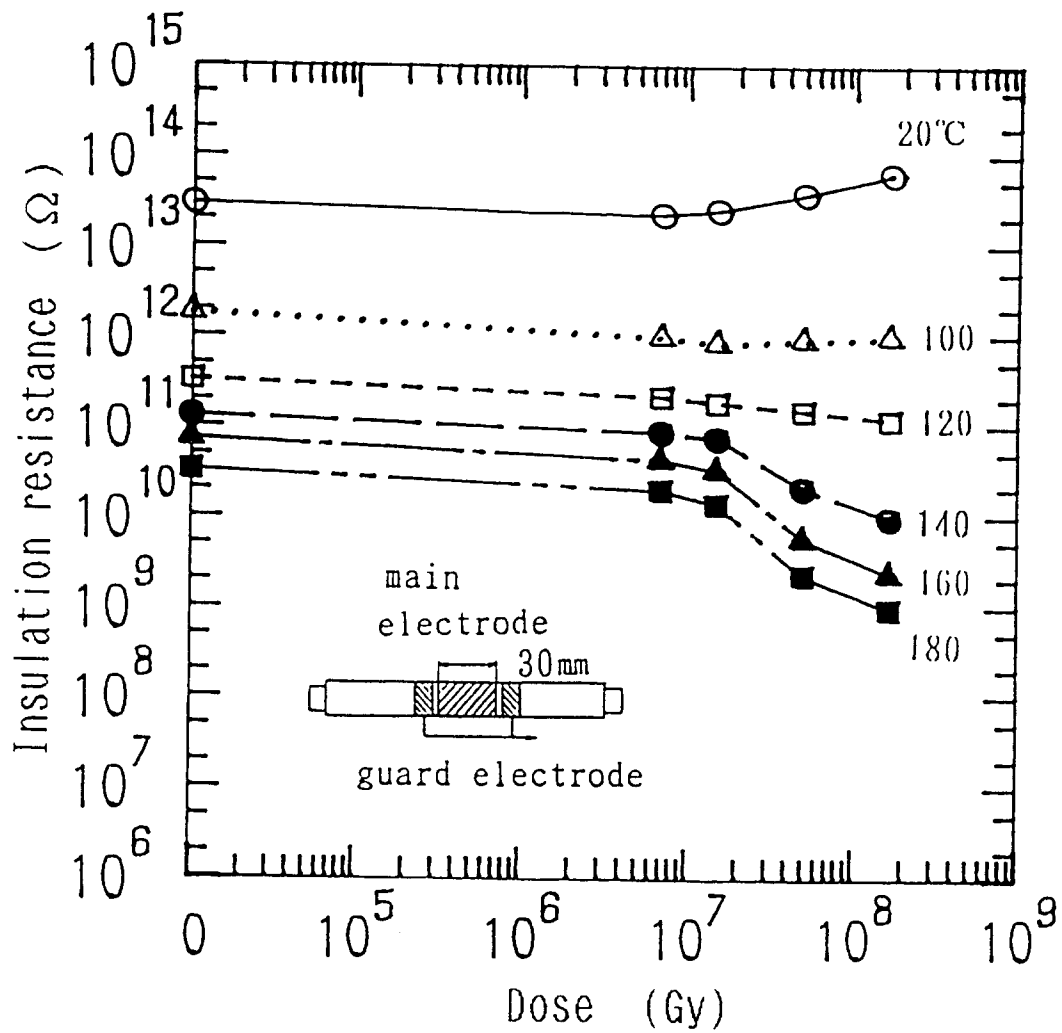


Fig.3 Insulation resistance vs. dose(type A).

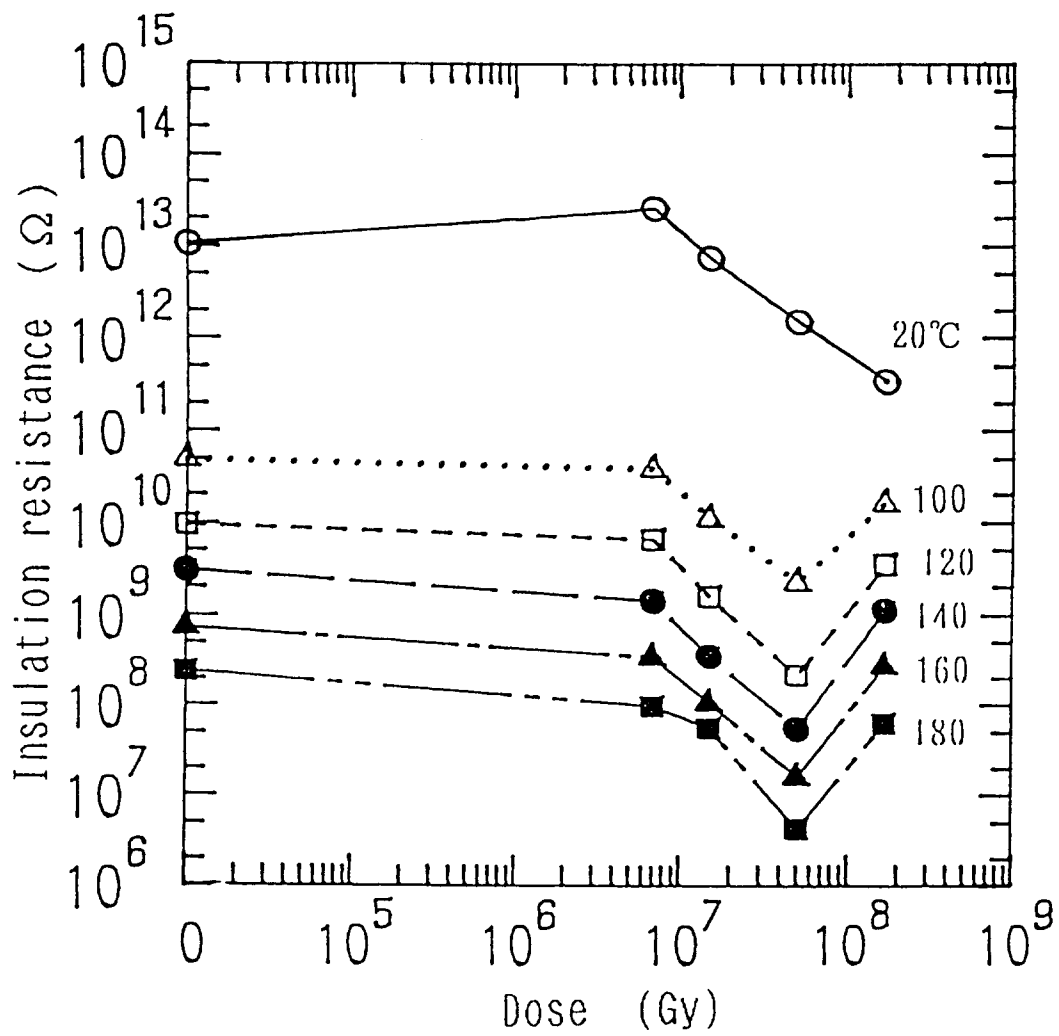


Fig.4 Insulation resistance vs. dose(type B).

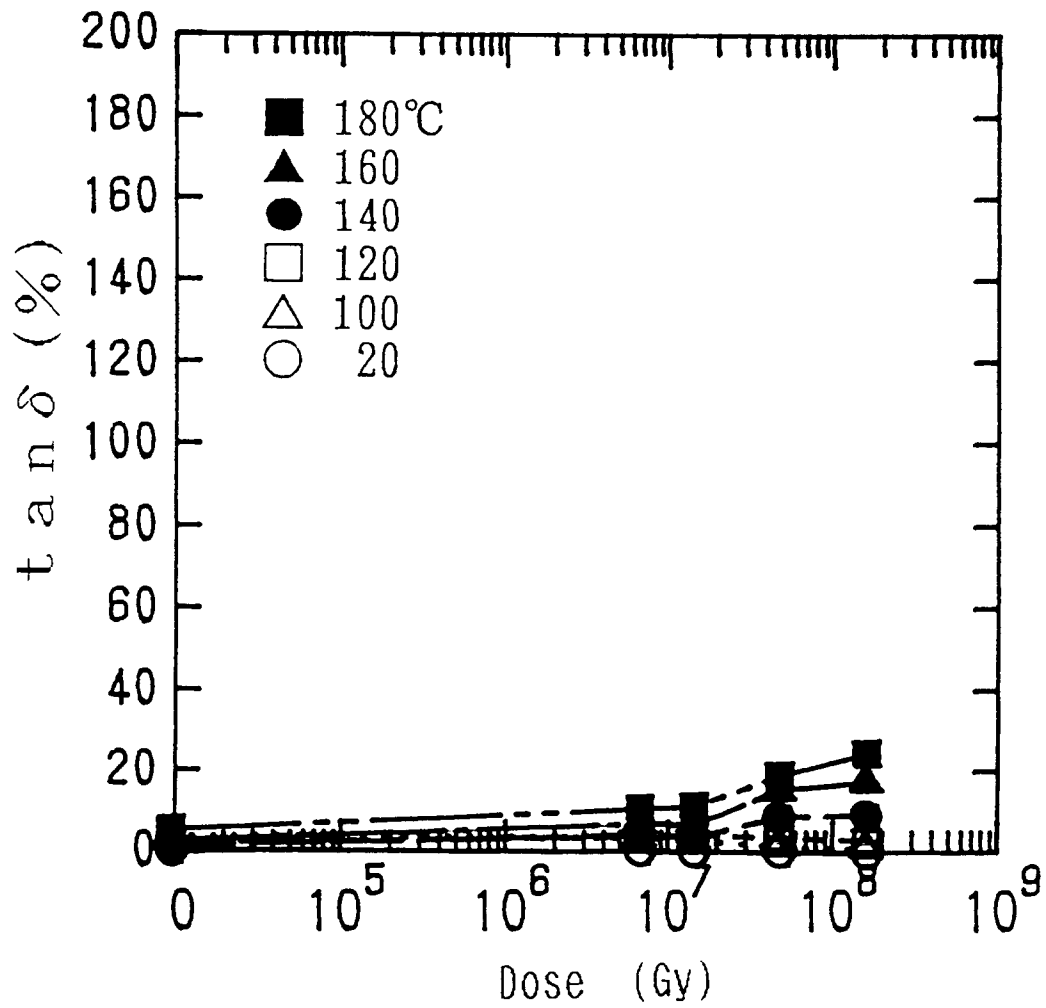


Fig.5 Tan δ of bar coils vs. dose(type A).

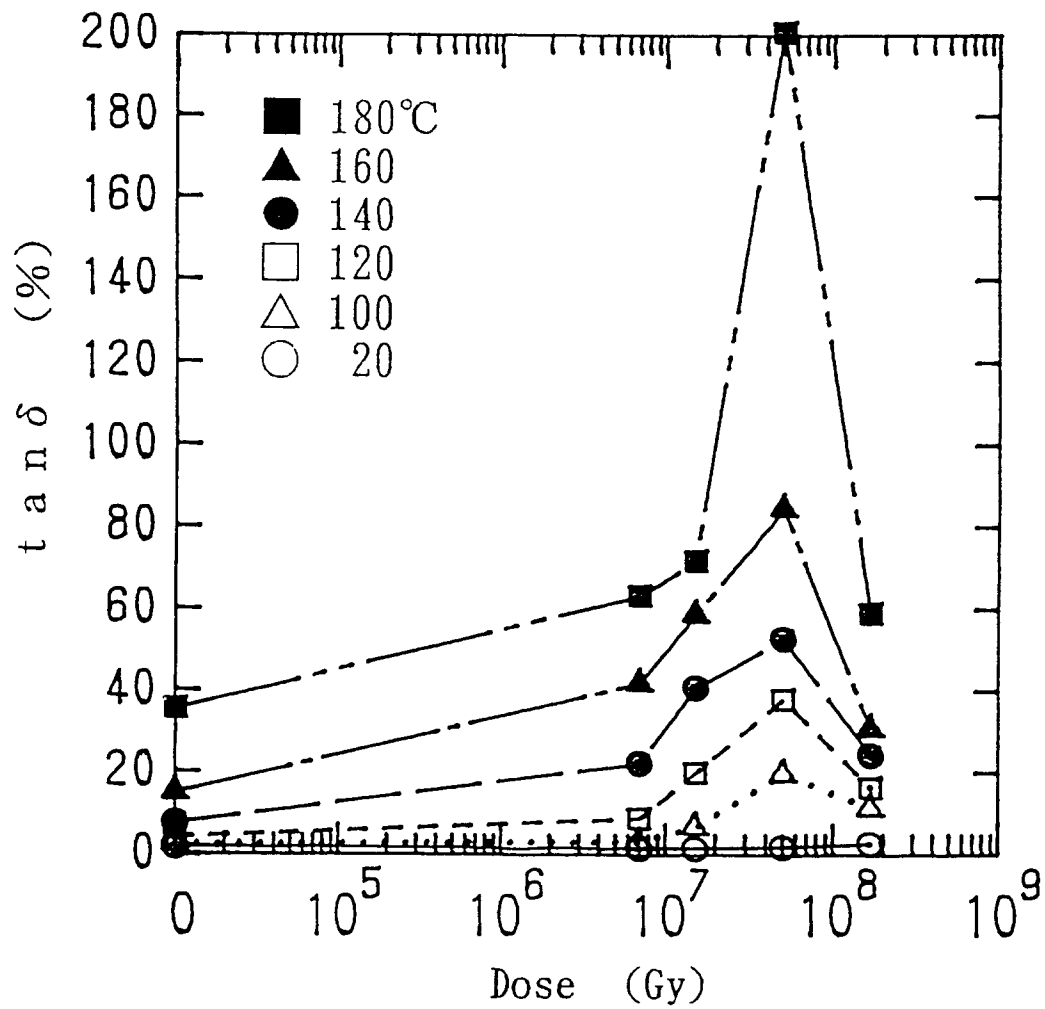


Fig.6 Tan δ of bar coils vs dose(type B).

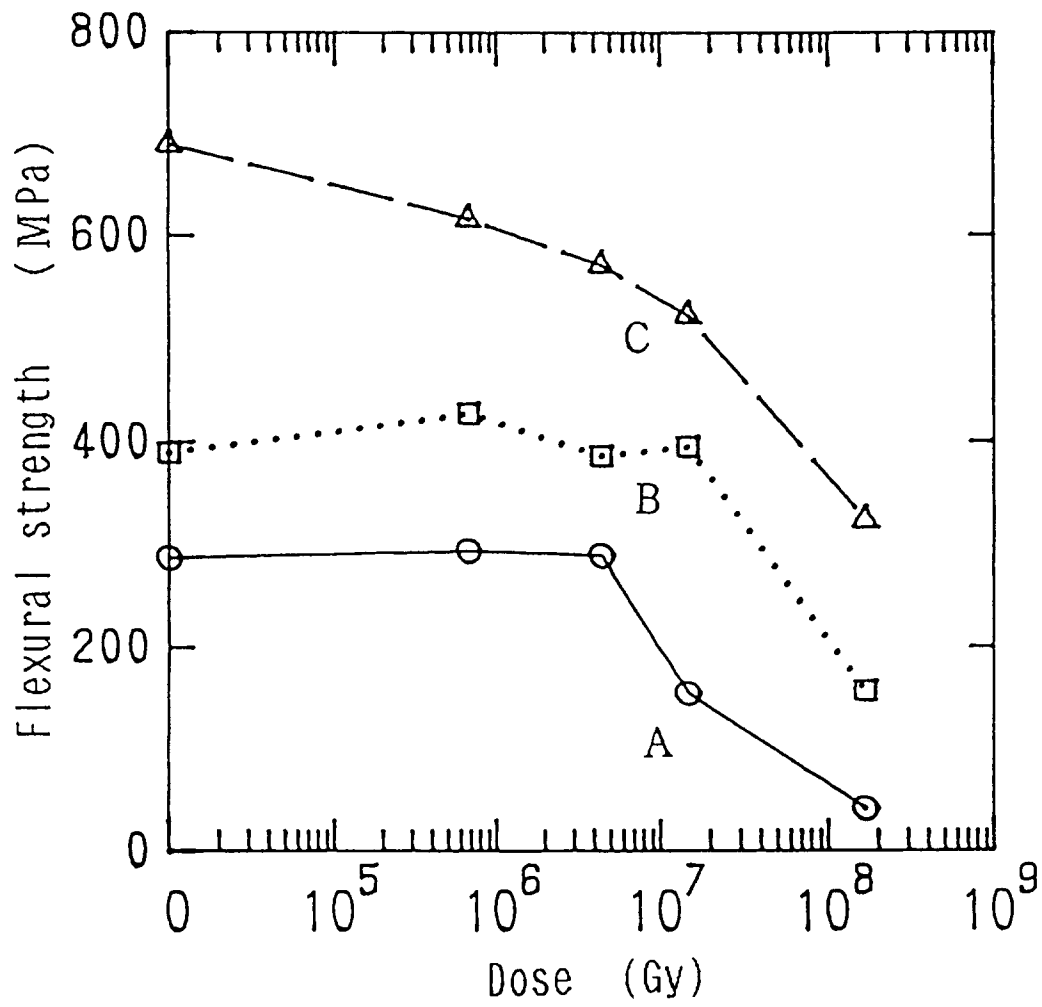


Fig.7 Flexural strength of laminates vs. dose.

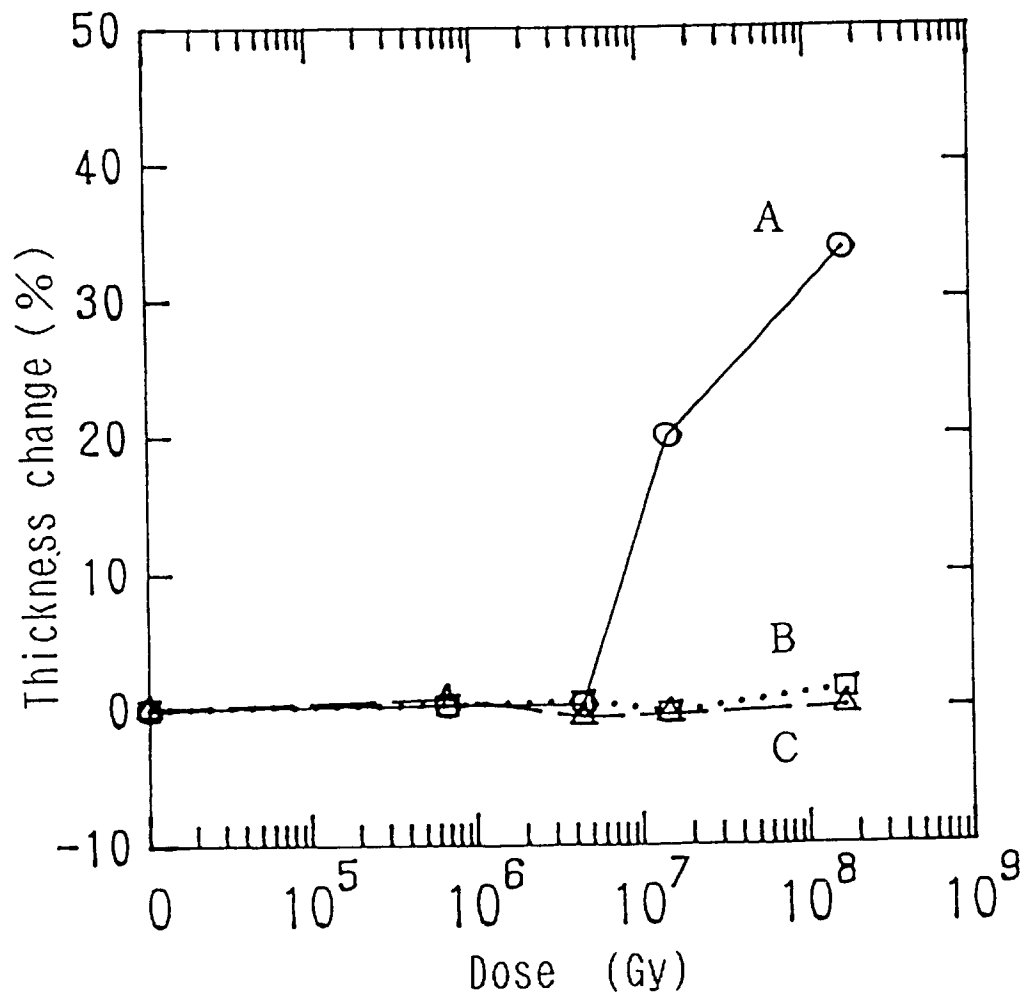


Fig.8 Thickness of laminates vs. dose.

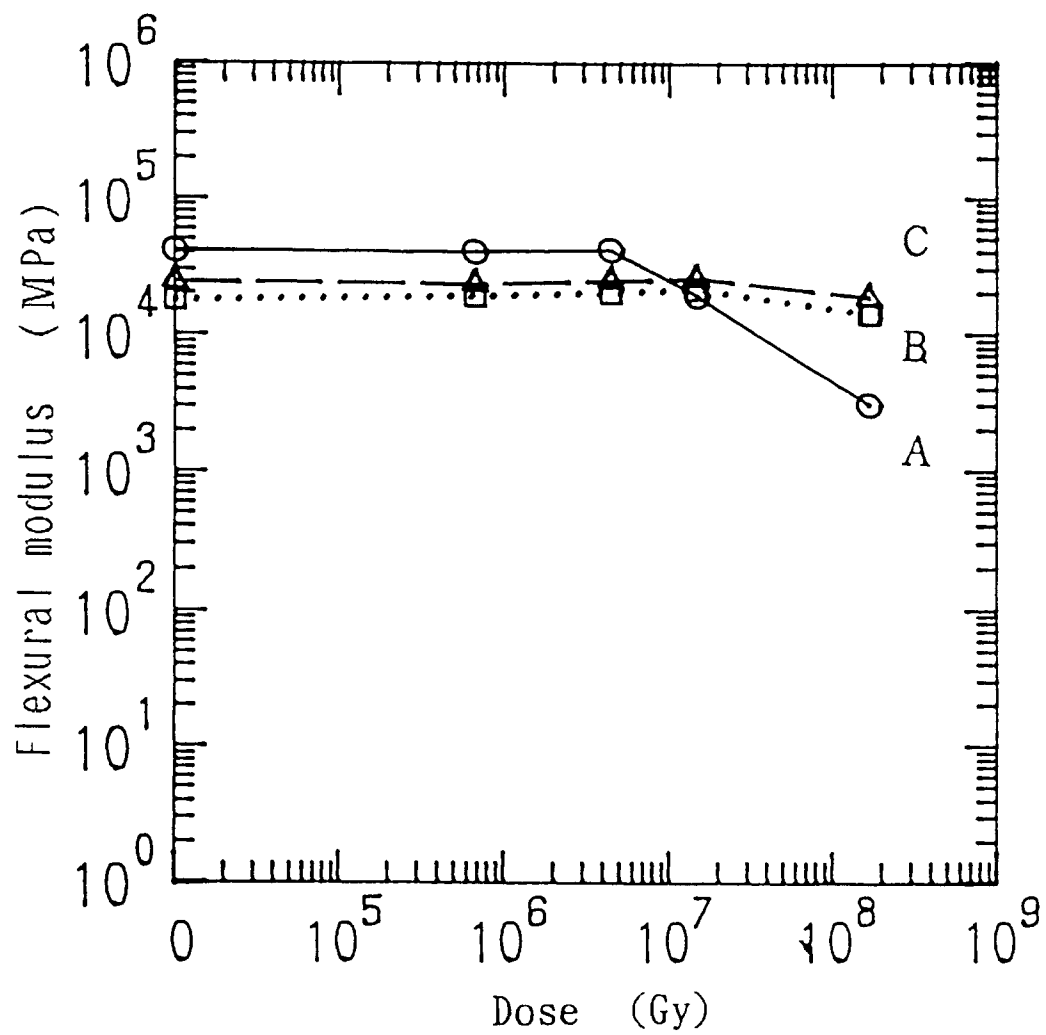
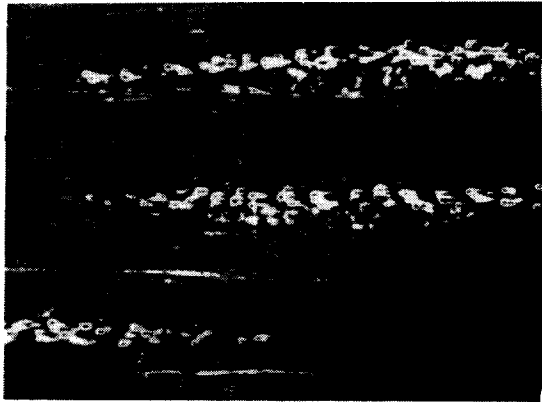


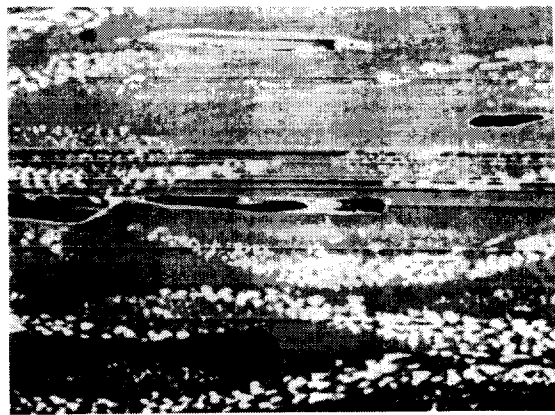
Fig.9 Flexural modulus of laminates vs. dose.



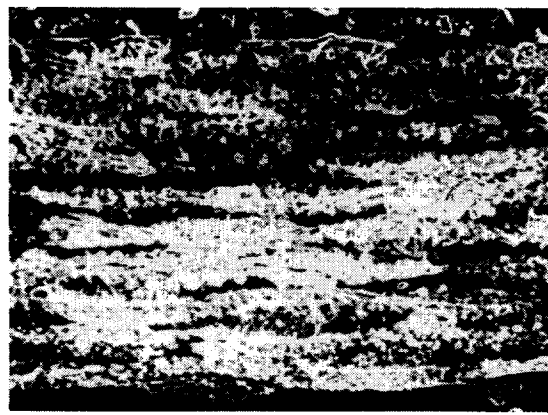
(a) un-irradiated sample (type A, $\times 200$)



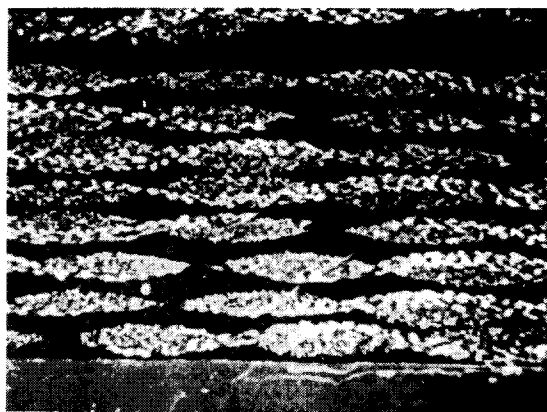
(b) 167MGy irradiated sample (type A, $\times 200$)



(c) un-irradiated sample (type B, $\times 60$)



(d) 167MGy irradiated sample (type B, $\times 60$)



(e) un-irradiated sample (type C, $\times 60$)



(f) 167MGy irradiated sample (type C, $\times 60$)

Fig.10 Cross-sectional photographs taken by a SEM

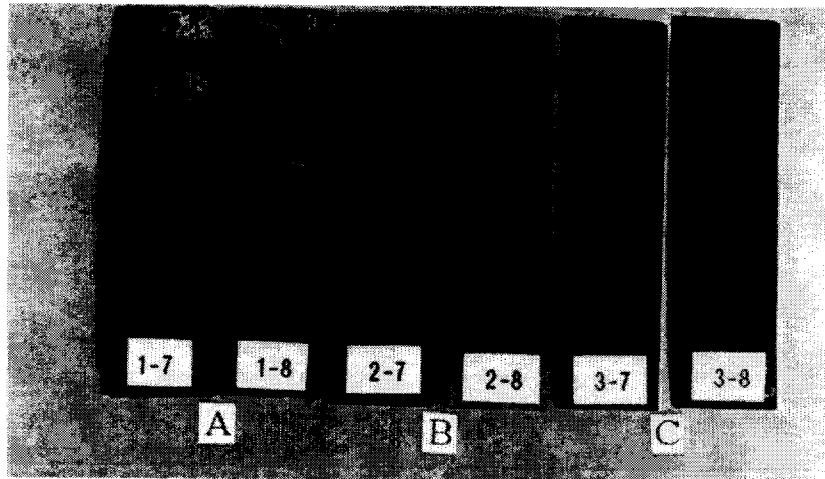


Fig.11 Appearance of laminates after 167 MGy irradiation.

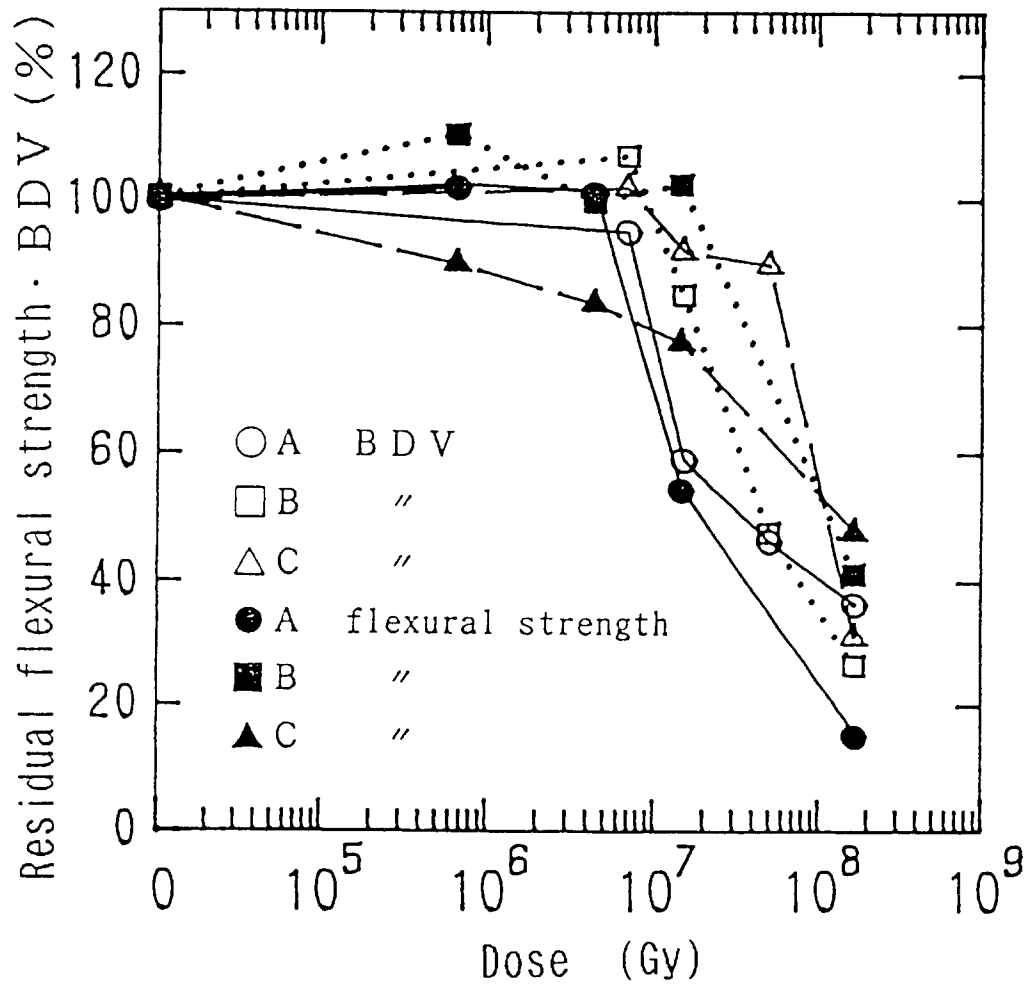


Fig.12 Residual BDV and flexural strength obtained from the results shown in Fig.1 and Fig.7.

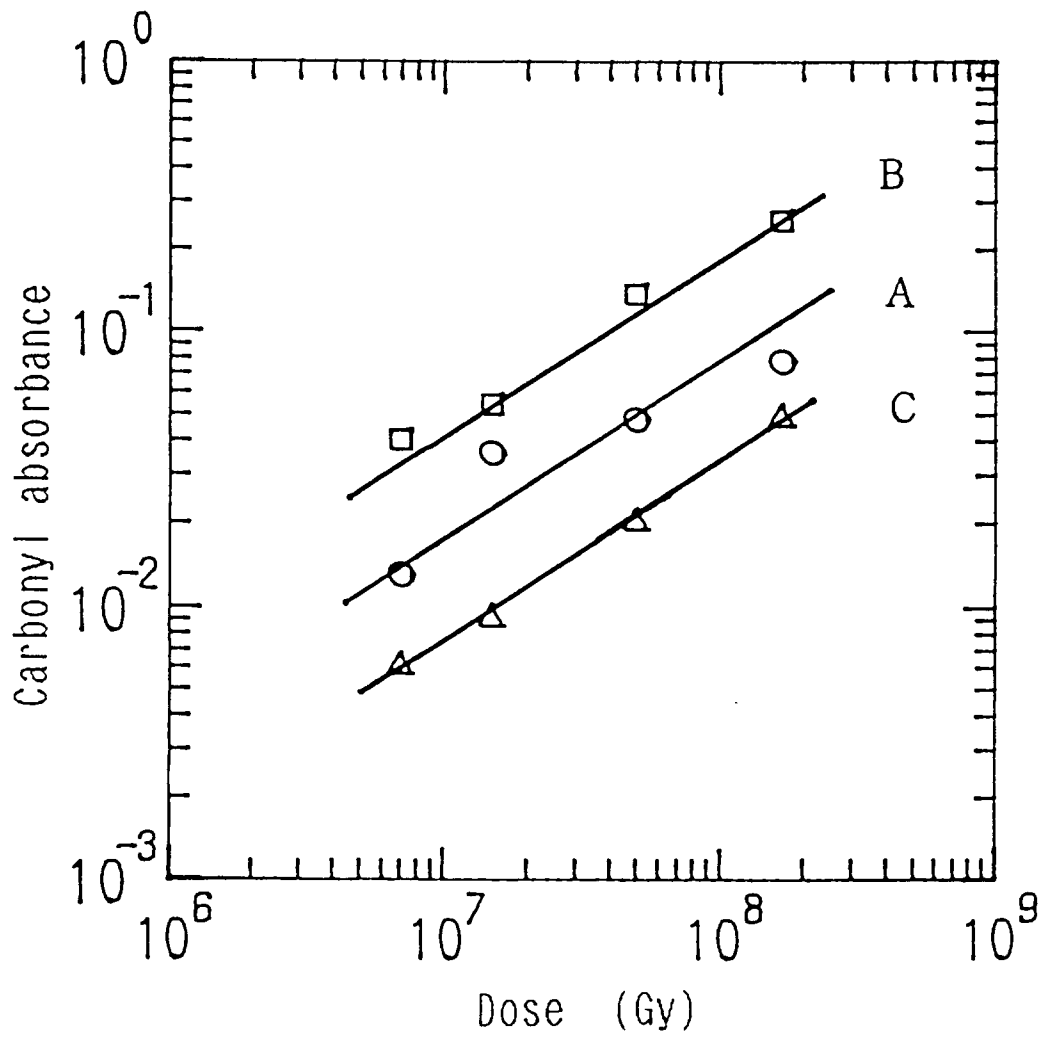


Fig.13 Carbonyl absorbance vs. dose.